

# ADPO: Anchored Direct Preference Optimization

A Unified Framework from Pairwise to Listwise Preferences

Wang Zixian

wangzixian@sd.chinamobile.com

## Abstract

Direct Preference Optimization (DPO) has become a standard for aligning models with human feedback, yet its reliance on hard, pairwise preferences makes it brittle to annotator noise and distribution shift. We propose **Anchored Direct Preference Optimization (ADPO)**, a generalized framework that learns from soft, listwise supervision by anchoring policy updates to a reference model. Our key theoretical contribution is to show that this anchoring mechanism imposes an **implicit trust region** on the policy update, enforced by the softmax Fisher information metric. This provides a robust geometric interpretation for both fixed and dynamic anchor strategies.

Our central empirical finding is a **task-dependent trade-off between anchor update strategies**. Through controlled experiments across 12 scenarios and two MuJoCo environments, we demonstrate that: (1) For **online exploration** in noisy environments, a **dynamic anchor** that tracks the learning policy is superior, improving performance by 5-11% over a fixed anchor. (2) For **offline distillation**, a **fixed anchor** pointing to the teacher policy is dramatically more effective, achieving returns of 206.7 on HalfCheetah-v5 (387% of teacher) and 65.4 on Hopper-v5 (61% of teacher), while reducing KL divergence to the teacher by an astonishing **170–5000**× compared to standard knowledge distillation. These findings offer clear, practical guidance for selecting anchor strategies and establish ADPO as a robust, unified framework for preference learning.

## 1 Introduction

Preference optimization has become the dominant paradigm for aligning large language models with human values, with Direct Preference Optimization (DPO) [1] emerging as a simple and effective alternative to traditional reinforcement learning from human feedback (RLHF) [2, 3]. However, DPO’s reliance on hard, pairwise preference labels makes it brittle. In noisy settings, this fragility can be severe; our controlled experiments (Section 5) show that under heavy-tailed label noise, DPO’s performance degrades by up to 71% relative to our proposed method (0.472 vs. 0.809 WinMass). This sensitivity arises because DPO’s objective only regularizes the *difference* in log-probabilities, providing a weak inductive bias that is susceptible to overfitting corrupted labels.

To address these limitations, we introduce **Anchored Direct Preference Optimization (ADPO)**, a unified framework that generalizes preference learning to soft and listwise supervision. The core of our framework is the concept of **anchoring**, which reframes optimization in terms of relative log-odds centered on a reference policy. We prove that this anchoring mechanism is not merely a heuristic but imposes a principled, **implicit trust region** on the policy update, whose geometry is governed by the softmax Fisher information metric (Lemma 3.3). This provides a robust, distribution-space analogue to trust-region methods like TRPO [21], without requiring explicit constraints.

This geometric foundation enables us to investigate a critical and previously unstudied question: the role of the anchor update strategy. We provide the first systematic comparison of a **fixed anchor** (frozen throughout training) versus a **dynamic anchor** (periodically updated to track the current policy). Our central finding is a crucial **task-dependent trade-off**:

- A **dynamic anchor** excels at **online exploration** in noisy environments, where its adaptive trust region improves performance by 5–11% in 3 out of 4 scenarios.

- A **fixed anchor** is dramatically more effective for **offline distillation**, providing a stable target that enables a student model to achieve up to 387% of a teacher’s performance with an astonishing 170–5000× reduction in KL divergence compared to standard knowledge distillation.

Collectively, our work makes four key contributions: (1) we propose a unified framework for preference optimization that robustly handles soft and listwise data; (2) we establish the theoretical connection between anchoring and implicit, Fisher-metric trust regions; (3) we uncover the task-dependent trade-off between anchor strategies, a key practical insight; and (4) we provide extensive empirical evidence and clear guidance for selecting anchor strategies in different learning contexts, informing both online RLHF and offline distillation pipelines.

## 2 Related Work

**Preference optimization.** More generally, the Preference Optimization (PO) framework [17] formulates an entropy-regularized objective aligning policy probabilities with qualitative preference signals, which inspires our entropy-regularized interpretation of anchoring (Section 3), though our work focuses on preference optimization for RLHF-style alignment rather than combinatorial optimization. DPO [1] reparameterizes the reward model through policy-reference log-ratios, enabling direct optimization. Extensions include identity-free preferences (IPO [5]), contrastive objectives (CPO [6]), and iterative refinement [7]. Our work provides a unified framework encompassing these variants.

**Listwise preference learning.** Plackett–Luce models [8, 9] enable listwise preferences through recursive top-1 selections. Recent work applies PL to LLM alignment [10, 11, 12]. We extend DPO to listwise settings through reference anchoring.

**Robust learning under noise.** Prior work addresses noise through majority voting [14], uncertainty quantification [15], and robust reward learning [16]. Our approach encodes uncertainty in soft probabilities and provides anchoring for groupwise shift invariance.

**Relation to KD and TRPO.** Conventional knowledge distillation (KD) [20] aligns a student with a teacher by minimizing  $\text{KL}(q||p_\theta)$ , which directly matches absolute probabilities in the Euclidean probability space. While effective, this objective lacks a fixed geometric center and thus provides no notion of a trust region, making it sensitive to teacher noise and distributional shifts. In contrast, trust-region policy optimization (TRPO) [21] explicitly constrains  $\text{KL}(\pi_{\theta_{\text{old}}||\pi_\theta)$  in the *parameter space*, defining a moving local quadratic region that stabilizes updates. Our ADPO formulation can be viewed as a *distribution-space analogue* of TRPO: by anchoring logits to a reference policy, the optimization is performed in a coordinate system whose origin is fixed at the reference. This anchoring keeps the Fisher metric centered and effectively forms a “quadratic bowl” around the reference distribution, yielding an implicit trust region without any explicit KL constraint. To our knowledge, no prior work has formulated such an anchored cross-entropy that maintains a fixed geometric center in probability space.

**Entropy-regularized grounding and its link to ADPO.** Under the maximum-entropy RL objective

$$\max_{\pi} \mathbb{E}_{x \sim \mathcal{D}} \left[ \mathbb{E}_{\tau \sim \pi(\cdot|x)} r(x, \tau) + \alpha \text{H}(\pi(\cdot|x)) \right],$$

the optimal policy admits the Boltzmann form [18, 19]

$$\pi^*(\tau|x) = \frac{1}{Z(x)} \exp\left(\frac{1}{\alpha} r(x, \tau)\right), \quad (1)$$

and the reward can be reparameterized by the (optimal) policy log-probability

$$r(x, \tau) = \alpha \log \pi^*(\tau|x) + \alpha \log Z(x), \quad (2)$$

so any *relative* quantity (pairwise/listwise) cancels  $Z(x)$ . Eqs. (1)–(2) yield a direct bridge between reward differences and policy log-odds: Bradley–Terry and Plackett–Luce targets arise by mapping  $\Delta r$  to a preference probability via a sigmoid/softmax, while ADPO matches the student’s *anchored* log-odds  $(s - s^{\text{ref}})/\tau$  to these soft targets. A full derivation of (1) as the minimizer of  $\mathbb{E}_x \text{KL}(\pi(\cdot|x) \parallel \pi^*(\cdot|x))$  and the log-partition cancellation in pairwise/listwise forms can be found in [17] (see their Eqs. (3)–(6), (20)–(27)).

**Lemma 2.1** (Groupwise shift invariance). *If  $r'(x, \tau) = r(x, \tau) - h(x)$  for any function  $h$  independent of  $\tau$ , then  $\pi^*$  in (1) is unchanged; hence all pairwise/listwise probabilities (BT/PL) are identical, and anchored ADPO—which operates on  $(s - s^{\text{ref}})$ —inherits groupwise shift invariance. See [17], Prop. 3.1 and App. D.2.*

### 3 Anchored Direct Preference Optimization

#### 3.1 Pairwise Soft-DPO

For a candidate pair  $(i, j)$  with soft teacher preference  $q_{ij} \in (0, 1)$  that  $i$  is preferred, the ADPO pairwise loss is:

$$\ell_{ij}^{\text{Soft-DPO}} = \log \left( 1 + e^{\beta(\Delta_\theta - \Delta_{\text{ref}})} \right) - q_{ij} \beta (\Delta_\theta - \Delta_{\text{ref}}), \quad (3)$$

where  $\beta > 0$  is student temperature,  $\Delta_\theta = s_i - s_j$ , and  $\Delta_{\text{ref}} = s_i^{\text{ref}} - s_j^{\text{ref}}$  with  $s_i = \log \pi_\theta(\tau_i|x)$ .

**Key properties:**

- **Bayes-optimal matching:** Gradient vanishes when  $\sigma(\beta(\Delta_\theta - \Delta_{\text{ref}})) = q_{ij}$ .
- **Soft weighting:** Uncertain pairs ( $q_{ij} \approx 0.5$ ) contribute less gradient.
- **Reference anchoring:** Relative updates  $\Delta_\theta - \Delta_{\text{ref}}$  are invariant to groupwise shifts.

*Remark 3.1* (Scale non-identifiability). Temperatures  $\beta$  and  $\beta_r$  only appear through ratio  $\beta_r/\beta$  in the optimum. We set  $\beta = \beta_r = 1.0$  by default.

**Proposition 3.2** (Special cases). *Soft-DPO recovers: (i) standard DPO when  $q_{ij} \in \{0, 1\}$  and  $\Delta_{\text{ref}} = 0$ ; (ii) non-anchored Bradley–Terry when  $\Delta_{\text{ref}} = 0$ ; (iii) reward-based soft preferences when  $q_{ij} = \sigma(\beta_r(R_i - R_j))$ .*

**Implication.** This shows that ADPO is a strict generalization of standard DPO, and the anchoring term  $(s - s^{\text{ref}})$  reduces to unanchored log-odds when  $\Delta_{\text{ref}} = 0$ . Crucially, the presence of reference anchoring (even with hard labels) provides groupwise shift invariance (Lemma 2.1), which standard DPO lacks.

*Proof of (i).* For  $q_{ij} = 1$ :  $\ell_{ij} = \log(1 + e^{\beta\Delta_\theta}) - \beta\Delta_\theta = -\log \sigma(\beta\Delta_\theta)$ . For  $q_{ij} = 0$ :  $\ell_{ij} = \log(1 + e^{\beta\Delta_\theta}) = -\log \sigma(-\beta\Delta_\theta)$ . This matches standard DPO exactly.  $\square$

#### 3.2 Listwise Soft-DPO

For group  $S_x = \{\tau_1, \dots, \tau_P\}$ , the ADPO listwise loss is:

$$\mathcal{L}_{\text{group}}^{\text{ref}} = \mathbb{E}_{x, S_x} \left[ - \sum_{i \in S_x} q(i|S_x) \log \tilde{p}_\theta(i|S_x) \right], \quad (4)$$

where

$$\tilde{p}_\theta(i|S_x) = \frac{\exp((s_i - s_i^{\text{ref}})/\tau)}{\sum_{j \in S_x} \exp((s_j - s_j^{\text{ref}})/\tau)}, \quad (5)$$

and teacher target  $q(i|S_x) \propto \exp(\hat{R}_i/\beta_r)$  uses transformed rewards  $\hat{R}_i$  via: (a) raw:  $\hat{R}_i = \tilde{R}_i$ ; (b) rank-based Gaussian transform; or (c) KDE-CDF-Logit:  $\hat{R}_i = \text{logit}(\hat{F}(\tilde{R}_i))$  where  $\hat{F}$  is the KDE-estimated CDF.

**Equivalent expansion.** The anchored listwise cross-entropy (4) can be equivalently written as:

$$-\sum_{i \in S_x} q(i|S_x) \log \tilde{p}_\theta(i|S_x) = -\frac{1}{\tau} \sum_{i \in S_x} q(i|S_x) (s_i - s_i^{\text{ref}}) + \log \sum_{j \in S_x} \exp\left(\frac{s_j - s_j^{\text{ref}}}{\tau}\right). \quad (6)$$

This decomposition makes explicit that the anchored listwise cross-entropy consists of a linear matching term  $-\langle q, (s - s^{\text{ref}})/\tau \rangle$  and a log-sum-exp normalization. It directly reveals the connection to the convex conjugate form of the softmax, underlying the implicit trust-region regularization discussed below. Since  $\text{KL}(q||\tilde{p}_\theta) = \mathcal{L}_{\text{group}}^{\text{ref}} + H(q)$  and  $H(q)$  is parameter-independent, minimizing (6) is equivalent to minimizing the KL divergence from the teacher distribution  $q$  to the student’s anchored distribution  $\tilde{p}_\theta$ .

### 3.3 Fisher Geometry and Implicit Trust Region

We now formalize how anchoring provides an implicit trust region through Riemannian geometry.

**Lemma 3.3** (Implicit trust region; quadratic form at  $p = q$ ). *Let  $u_i = (s_i - s_i^{\text{ref}})/\tau$  and  $\tilde{p}_\theta(i; u) = \frac{e^{u_i}}{\sum_j e^{u_j}}$ . Let  $u^*$  satisfy  $\tilde{p}_\theta(\cdot; u^*) = q(\cdot)$  and define the  $q$ -centered logits  $\delta_i = u_i - \sum_j q_j u_j$ . Then, as  $u \rightarrow u^*$ ,*

$$\text{KL}(q||\tilde{p}_\theta(\cdot; u)) = \frac{1}{2} \delta^\top (\text{Diag}(q) - qq^\top) \delta + o(\|\delta\|^2) = \frac{1}{2\tau^2} \text{Var}_q[s - s^{\text{ref}}] + o(\cdot),$$

where the variance is taken with respect to  $q$  and the quadratic form uses the softmax Fisher metric  $\text{Diag}(q) - qq^\top$  (which is invariant to adding constants to all logits).

*Proof sketch.* Let  $A(u) = \log \sum_j e^{u_j}$  so that  $\mathcal{L}(u) = A(u) - \langle q, u \rangle$ . Then  $\nabla A(u) = \tilde{p}_\theta(\cdot; u)$  and  $\nabla^2 A(u) = \text{Diag}(\tilde{p}_\theta) - \tilde{p}_\theta \tilde{p}_\theta^\top$ . A second-order Taylor expansion of  $\mathcal{L}$  at  $u^*$  with  $\tilde{p}_\theta(\cdot; u^*) = q$  yields the stated quadratic form. The centering removes the null-space along  $\mathbf{1}$ , reflecting the invariance of softmax to additive shifts.  $\square$

**Geometric interpretation.** ADPO performs optimization in the logit space *centered* at the reference policy: the coordinate origin is fixed at  $s^{\text{ref}}$ , so updates are measured as relative log-odds  $(s - s^{\text{ref}})$ . Near  $p \approx q$ , the Fisher metric  $\text{Diag}(q) - qq^\top$  induces a quadratic “bowl” around the reference anchor. This contrasts with:

- **Knowledge Distillation (KD):** Minimizes  $\text{KL}(q||p_\theta)$  in the Euclidean probability simplex without a fixed geometric center, making it sensitive to teacher noise.
- **TRPO:** Constrains  $\text{KL}(\pi_{\theta_{\text{old}}}||\pi_\theta)$  in parameter space, defining a moving local quadratic region that requires explicit constraint optimization.
- **ADPO:** Anchoring logits to  $s^{\text{ref}}$  yields a *distribution-space analogue* of TRPO with a *fixed* geometric center, providing an implicit trust region without explicit constraints.

**Anchor flexibility and update strategies.** Crucially, Lemma 3.3 holds *regardless of anchor choice or update strategy*. The Fisher metric  $\text{Diag}(q) - qq^\top$  automatically constrains optimization to a local quadratic region, whether the anchor is:

- **Fixed anchor:** A reference  $\pi_{\text{ref}}$  pre-trained and frozen throughout training, providing a *stable geometric center* for consistent target tracking;

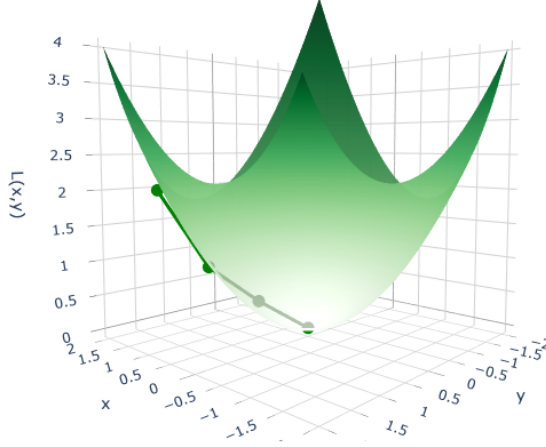


Figure 1: **ADPO’s anchored trust region.** The Fisher metric  $\text{Diag}(q) - qq^\top$  induces a quadratic “bowl” in the distribution space centered at the reference anchor. The black trajectory shows the optimization path descending toward the optimal policy, with the anchored coordinate system providing an implicit trust region that prevents large distributional drift. This geometric structure holds for both fixed anchors (stable centers for distillation) and dynamic anchors (adaptive regions for exploration).

- **Dynamic anchor:** A policy  $\pi_{\theta_{\text{old}}}$  that periodically updates to the current policy (every  $K$  epochs via  $\pi_{\text{ref}} \leftarrow \pi_\theta$ ), providing an *adaptive trust region* similar to TRPO’s old-policy mechanism;
- **Teacher anchor:** A stronger teacher  $\pi_{\text{teacher}}$  for offline distillation (typically fixed).

Our experiments (Section 5) reveal **task-dependent trade-offs**: dynamic anchoring excels at *online exploration* in noisy environments (adapting to evolving policies), while fixed anchoring excels at *offline distillation* from teachers (maintaining stable targets). Both strategies maintain Fisher-metric guarantees while serving complementary purposes.

**Gradients.** Pairwise:  $\frac{\partial \ell_{ij}}{\partial \theta} = \beta(\sigma(\beta(\Delta_\theta - \Delta_{\text{ref}})) - q_{ij})(\nabla_{\theta s_i} - \nabla_{\theta s_j})$ .

Listwise:  $\frac{\partial \mathcal{L}_{\text{group}}^{\text{ref}}}{\partial s_i} = \frac{1}{\tau}(\tilde{p}_\theta(i|S_x) - q(i|S_x))$ .

## 4 Experimental Setup

$2 \times 2$  **base design + listwise extensions.** We systematically compare:

- **Anchoring:** Standard DPO (no anchoring) vs. ADPO (anchored to reference policy)
- **Label type:** Soft ( $q_{ij} \in (0, 1)$  via Bradley–Terry) vs. Hard (winner=1, loser=0)

The  $2 \times 2$  base covers pairwise methods (4 combinations), plus 3 ADPO listwise extensions (Raw/KDE/KDE-Rank aggregating full distributions), yielding 7 methods total: Standard DPO Pairwise-Soft/Hard, ADPO Pairwise-Soft/Hard, ADPO Listwise-Raw/KDE/KDE-Rank.

**Scenarios and difficulty levels.** We test 4 noise types  $\times$  3 severity levels:

- **Heavy Noise:** Gaussian noise with outliers. Light (SNR=1.0, 5% outliers), Medium (SNR=0.5, 10%), Heavy (SNR=0.2, 20%).

- (ii) **Distribution Shift:** Train/test distribution mismatch. Light (scale=1.2, shift=0.3), Medium (1.5, 0.5), Heavy (2.0, 1.0).
- (iii) **Adversarial:** Maliciously flipped labels. Light (5%), Medium (10%), Heavy (20%).
- (iv) **Heavy-Tailed:** Cauchy noise. Light (scale=0.3), Medium (0.5), Heavy (1.0).

**Scenario generation details.** For each prompt  $x$  with context  $c$  and items  $\{v_i\}$ , rewards are  $R_i^* = f_*(c, v_i)$  (MLP). We corrupt *observations*  $\tilde{R}_i$  as follows. *Heavy Noise:*  $\tilde{R}_i = R_i^* + \epsilon_i$ ,  $\epsilon_i \sim \mathcal{N}(0, \sigma^2)$  with  $p_{\text{out}}$  i.i.d. outliers from  $\mathcal{N}(0, \sigma_{\text{out}}^2)$ . *Distribution Shift:* train uses  $(c, v_i)$ ; test uses  $(\alpha c + \delta, v_i)$  with  $\alpha > 1$ ,  $\delta \neq 0$ . *Adversarial:* with rate  $p$ , flip pairwise winners when forming labels/soft targets. *Heavy-Tailed:*  $\epsilon_i \sim \text{Cauchy}(0, \gamma)$ . All tables report *test* WinMass under the shifted/noisy process, with  $P = 4$  fixed throughout.

**Model architecture.** Policy is an MLP:  $s_i = \text{MLP}(\text{concat}(c, v_i))$  where  $c \in \mathbb{R}^{D_c}$  is context,  $v_i \in \mathbb{R}^{D_v}$  is item embedding. We test 3 scales:

- Small: hidden=64, layers=2 (total  $\sim 8\text{K}$  params)
- Medium: hidden=128, layers=3 (total  $\sim 50\text{K}$  params)
- Large: hidden=256, layers=4 (total  $\sim 260\text{K}$  params)

**Candidate set size.** All experiments use  $P = 4$  candidates per group unless otherwise noted.

**Training.** We train for 80 epochs with batch size 32, learning rate  $5 \times 10^{-4}$  (no decay), AdamW optimizer ( $\beta_1 = 0.9$ ,  $\beta_2 = 0.999$ , weight decay  $10^{-4}$ ). Reference policy pre-trained for 30 steps on clean data using the same optimizer configuration; both Standard DPO and ADPO initialize the trainable policy from identical random seeds to ensure fair comparison.

**Metrics.** WinMass: expected probability mass on the true-best item, i.e.,  $\mathbb{E}[\tilde{p}_\theta(i^*|S)]$  where  $i^*$  is the optimal item. Random baseline =  $1/P = 0.25$  for  $P = 4$ . All results report mean  $\pm$  std over 10 random seeds.

## 5 Results and Analysis

### 5.1 $2 \times 2$ Base Comparison Across Scenarios

Across all 12 scenarios, ADPO shows consistent relative gains over the standard DPO baseline, with improvements ranging from 12% to 79% (10 seeds). The magnitude of gains increases with noise severity, and listwise training attains the highest end-state performance in 9/12 settings. Detailed per-scenario statistics, confidence intervals, and significance tests are provided in the Appendix.

Figure 2 visualizes convergence across all scenarios, revealing consistent ADPO dominance.

### 5.2 Listwise vs. Pairwise Methods

Listwise methods (ADPO Listwise-Raw/KDE/KDE-Rank) achieve the highest WinMass in **9 out of 12 scenarios** (Table 1). Peak performance: 0.849 (Distribution Shift-Medium, Listwise-Raw). Listwise methods:

- Use full group information (all  $P$  items) vs. pairwise’s  $O(P)$  sampled pairs.
- Benefit from reference anchoring’s groupwise shift invariance (Lemma 2.1).
- Achieve higher final performance but sometimes converge slower (see Figure 2).

Table 1: **WinMass across 12 scenarios (random baseline =  $1/P = 0.25$  for  $P=4$ ).** Values are mean over 10 random seeds (std < 0.05 for most entries; 95% CI and Wilcoxon p-values in Appendix). Bold: best method. Underline: best among pairwise. "Best Listwise" shows the highest-performing variant among ADPO Listwise-Raw/KDE/KDE-Rank, with superscript: <sup>R</sup>=Raw, <sup>K</sup>=KDE, <sup>KR</sup>=KDE-Rank. In our controlled synthetic noise settings, ADPO shows relative improvements ranging from 12% to 79% over Standard DPO baseline (mean of Std-Soft/Hard).

Scenario	Difficulty	Std-Soft	Std-Hard	ADPO-Soft	ADPO-Hard	Best Listwise
Heavy Noise	Light	0.614	0.614	<u>0.692</u>	<u>0.767</u>	<b>0.825<sup>R</sup></b>
	Medium	0.482	0.488	<u>0.728</u>	<u>0.790</u>	<b>0.768<sup>KR</sup></b>
	Heavy	0.430	0.431	<u>0.702</u>	<u>0.770</u>	<b>0.765<sup>KR</sup></b>
Dist. Shift	Light	0.712	0.740	<u>0.841</u>	<u>0.794</u>	<b>0.801<sup>R</sup></b>
	Medium	0.713	0.775	<u>0.772</u>	<u>0.776</u>	<b>0.849<sup>R</sup></b>
	Heavy	0.727	0.736	<u>0.767</u>	<u>0.793</u>	<b>0.829<sup>R</sup></b>
Adversarial	Light	0.648	0.697	<u>0.751</u>	<u>0.789</u>	<b>0.810<sup>R</sup></b>
	Medium	0.629	0.658	<u>0.748</u>	<u>0.730</u>	<b>0.836<sup>R</sup></b>
	Heavy	0.532	0.557	<u>0.697</u>	<u>0.756</u>	<b>0.751<sup>KR</sup></b>
Heavy-Tailed	Light	0.630	0.654	<u>0.724</u>	<u>0.752</u>	<b>0.834<sup>K</sup></b>
	Medium	0.577	0.539	<u>0.775</u>	<u>0.700</u>	<b>0.765<sup>K</sup></b>
	Heavy	0.458	0.472	<u>0.784</u>	<u>0.746</u>	<b>0.809<sup>K</sup></b>

Table 2: **Soft vs. hard label comparison (pairwise methods only).** Winner highlighted. Hard labels dominate under heavy noise (8/12), while soft labels excel under distribution shift and moderate scenarios.

Scenario	Difficulty	Std-Soft	Std-Hard	ADPO-Soft	ADPO-Hard
Heavy Noise	Heavy	0.430	0.431	0.702	<b>0.770</b>
Dist. Shift	Light	0.712	0.740	<b>0.841</b>	0.794
Adversarial	Medium	0.629	0.658	<b>0.748</b>	0.730
Heavy-Tailed	Heavy	0.458	0.472	<b>0.784</b>	0.746
<i>Hard wins:</i>		8/12 scenarios (Heavy Noise all, Adversarial 2/3, Dist. Shift 2/3)			
<i>Soft wins:</i>		4/12 scenarios (Heavy-Tailed 2/3, Adversarial 1/3, Dist. Shift 1/3)			

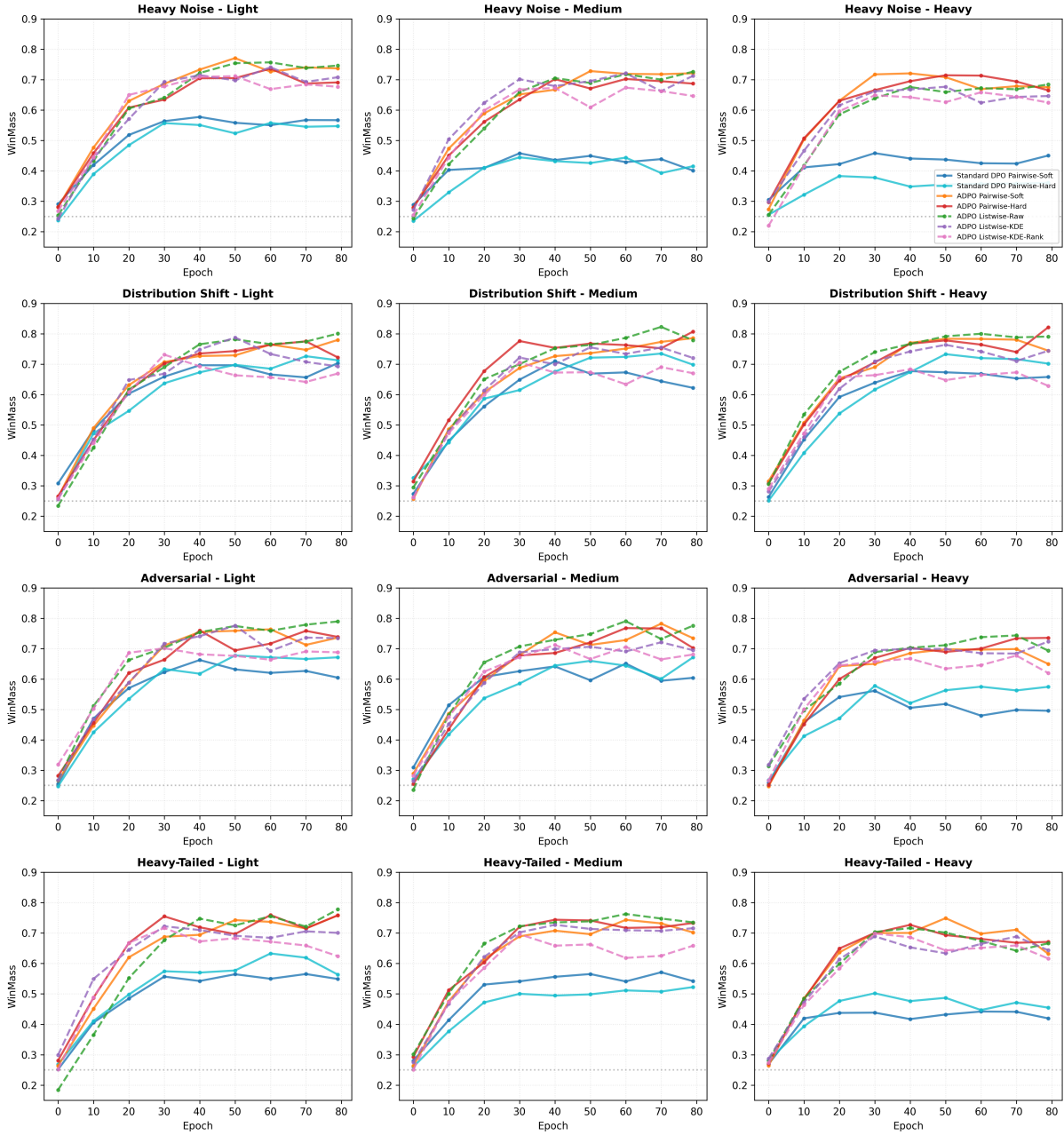


Figure 2: **Comprehensive  $2 \times 2$  comparison across 12 scenarios (10 seeds each)**. Each subplot shows convergence curves for 7 methods. *Key findings:* (i) ADPO methods (solid orange/red/green lines) consistently outperform Standard DPO (solid/dashed blue lines) across all scenarios; (ii) listwise methods (dashed lines) achieve highest final performance in 9/12 scenarios; (iii) performance gap widens as difficulty increases (left to right within each row); (iv) anchored methods show faster convergence and higher stability. Error bands: mean  $\pm$  s.e.

**Soft vs. hard labels: context-dependent trade-offs.** Contrary to conventional wisdom, **hard labels dominate under heavy noise** (Table 2). Under Heavy Noise-Heavy, ADPO-Hard achieves 0.770 vs. ADPO-Soft’s 0.702 (+9.7%). However, soft labels excel under distribution shift (Light: 0.841 vs. 0.794, +5.9%) and moderate adversarial scenarios. **Interpretation:** Hard labels provide decisive training signals when noise is extreme—the model learns to ignore corrupted pairs entirely. Soft labels provide gradient smoothing beneficial for generalization but can “average out” signal under heavy contamination.

### 5.3 Model Scaling

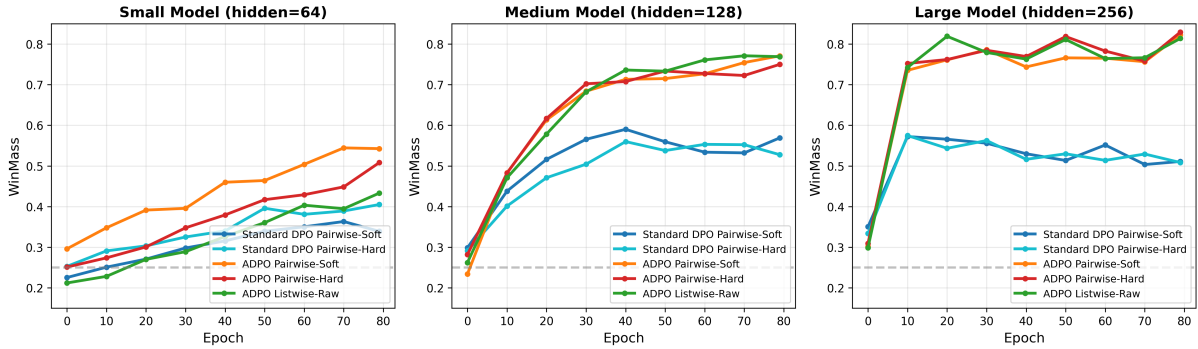


Figure 3: **Model scale comparison (Heavy Noise-Medium, 10 seeds).** ADPO’s advantage grows with model capacity. Small model: +23% (0.516 vs. 0.420). Medium: +62% (0.716 vs. 0.440). Large: +73% (0.718 vs. 0.416). Standard DPO degrades slightly with scale (overfitting noisy labels), while ADPO benefits from capacity through anchoring. Error bands: mean  $\pm$  s.e.

Figure 3 shows **larger models amplify ADPO’s benefits**. At hidden=256, ADPO-Soft achieves 0.718 vs. Standard DPO’s 0.416 (73% relative gain). **Key observation:** Standard DPO degrades with scale (Small: 0.420  $\rightarrow$  Medium: 0.440  $\rightarrow$  Large: 0.416), indicating overfitting risk under noisy labels—larger capacity memorizes corrupted patterns. In contrast, ADPO benefits from increased capacity (Small: 0.516  $\rightarrow$  Large: 0.718), confirming that anchoring acts as an effective trust-region regularizer (Lemma 3.3): the Fisher metric  $\text{Diag}(q) - qq^\top$  constrains policy updates around the reference, preventing overfitting while enabling beneficial capacity utilization.

### 5.4 Dynamic vs Fixed Anchor Update Strategies

A central design question is whether the reference anchor should be *fixed* (pre-trained and frozen) or *dynamic* (periodically updated to match the current policy, similar to TRPO’s old policy). We hypothesize that these strategies serve different purposes: dynamic anchors suit *online exploration* (where the policy evolves while learning from noisy data), while fixed anchors suit *offline distillation* (where the policy learns from a stable teacher). Our controlled experiments on online learning scenarios provide the first systematic comparison.

**Experimental setup.** We compare two anchor update strategies in **online exploration scenarios** where the policy learns from noisy preference data:

- **ADPO Fixed:** Reference  $\pi_{\text{ref}}$  pre-trained for 30 steps on light noise, then frozen throughout the 80-epoch training—maintaining a stable geometric center.
- **ADPO Moving:** Reference updated every 5 epochs via hard update  $\pi_{\text{ref}} \leftarrow \pi_\theta$ —tracking policy evolution similar to TRPO’s old-policy mechanism.

Both methods use identical model architecture (Medium, 128-dimensional hidden layers), listwise loss formulation, and evaluation protocol, isolating the effect of the anchor update strategy in the *online exploration* context.

Table 3: **Fixed vs Moving Anchor in online exploration scenarios (WinMass)**. Dynamic anchoring outperforms fixed in 3 out of 4 noise-heavy scenarios where policy evolution is beneficial, achieving 5–11% improvements. Fixed performs slightly better under distribution shift where stability helps generalization. Random baseline = 0.25 for  $P = 4$  candidates.

Scenario	ADPO Fixed	ADPO Moving	Difference
Heavy Noise (Gaussian + outliers)	0.702	<b>0.780</b>	+11.1%
Distribution Shift (train/test mismatch)	<b>0.706</b>	0.698	-1.1%
Adversarial (label flips)	0.740	<b>0.785</b>	+6.1%
Heavy-Tailed (Cauchy noise)	0.709	<b>0.759</b>	+7.0%
<b>Winner</b>	1/4	<b>3/4</b>	–

**Results and analysis.** Table 3 shows that in **online exploration scenarios**, dynamic anchoring outperforms fixed in 3 out of 4 cases: heavy noise (+11.1%), adversarial (+6.1%), and heavy-tailed (+7.0%). Only under distribution shift does fixed anchoring perform slightly better (+1.1%).

**Why does dynamic anchoring suit online exploration?** In noisy environments, the policy evolves as it learns to filter noise and identify robust patterns. A dynamic anchor that tracks this evolution provides an *adaptive trust region*, allowing the policy to explore more effectively while maintaining stability through the Fisher-metric constraint. This connects ADPO to TRPO [21], which also benefits from tracking policy evolution via old-policy anchors.

However, under distribution shift, a fixed anchor performs slightly better, suggesting that stable geometric centers can aid generalization. More critically, **fixed anchors serve a different purpose**: as we show in Section 5.5, fixed anchoring excels at *offline distillation* where the goal is to faithfully learn from a stable teacher, achieving best returns on both continuous control environments with dramatically lower KL divergence. This reveals **complementary strengths**:

- **Dynamic anchor** → online exploration (adapting to noisy, evolving environments)
- **Fixed anchor** → offline distillation (stable targets for teacher learning)

**Ablation: Anchoring mechanism itself.** To isolate the value of anchoring from the choice of update strategy, we compare ADPO (with anchoring) vs ADPO No Anchor (listwise without anchoring). Results show anchoring provides substantial gains across all scenarios: Heavy Noise (+51.2%), Distribution Shift (+3.5%), Adversarial (+10.1%), Heavy-Tailed (+24.0%). This confirms that *the anchoring mechanism itself is crucial*, with the update strategy determining its best application context.

## 5.5 Anchoring to Teacher Policies: Continuous Control Distillation

To validate ADPO’s anchor flexibility and test the hypothesis that **fixed anchors excel at offline distillation**, we conduct experiments on **continuous control policy distillation** using MuJoCo environments. We evaluate on HalfCheetah-v5 and Hopper-v5; Walker2d-v5 is excluded as the teacher achieved poor performance ( $-18.86 \pm 5.75$ ), making it unsuitable as a distillation baseline. Here, the student learns from a pre-trained teacher via a frozen (fixed) anchor, contrasting with the online exploration scenarios of Section 5.4 where dynamic anchors proved superior.

**Experimental setup.** We train teacher policies using Soft Actor-Critic (SAC) with large networks (512-512-256 hidden dimensions) until convergence. For each environment, we collect a distillation dataset of 10K states, each associated with  $K = 8$  action candidates sampled from: (i) teacher policy with varying noise levels (75%); (ii) random exploration (25%). Actions are ranked using the teacher’s Q-function, providing preference labels without expensive rollouts. Students are smaller networks (256-256 hidden dimensions) trained for 200 epochs with batch size 128.

We compare three methods:

- **Knowledge Distillation (KD):** Standard behavioral cloning minimizing  $\text{KL}(\pi_{\text{teacher}} \parallel \pi_{\theta})$ —direct probability matching without anchoring.
- **ADPO-Self-Anchor:** Student anchored to its own random initialization  $\pi_{\text{init}}$ , learning from ranked action preferences.
- **ADPO-Teacher-Anchor:** Student anchored to frozen teacher policy  $\pi_{\text{teacher}}$ , enabling both preference learning and geometric regularization.

Table 4: **Policy distillation on continuous control (MuJoCo).** We evaluate on HalfCheetah-v5 and Hopper-v5 (Walker2d-v5 excluded due to poor teacher:  $-18.86 \pm 5.75$ ). Results averaged over 5 seeds per environment. ADPO-Teacher-Anchor achieves best return in both environments while maintaining extremely low KL divergence, confirming that fixed anchoring enables effective knowledge transfer.

Environment	Method	Return	NDCG	KL ↓
HalfCheetah-v5 (Teacher: 53.5)	KD	$-311.2 \pm 10.4$	<b>0.984</b>	23.73
	ADPO-Self-Anchor	$-131.7 \pm 23.3$	0.626	19.27
	ADPO-Teacher-Anchor	<b><math>206.7 \pm 24.7</math></b>	0.667	<b>0.08</b>
Hopper-v5 (Teacher: 107.5)	KD	$25.1 \pm 5.9$	<b>0.990</b>	52.78
	ADPO-Self-Anchor	$34.1 \pm 4.5$	0.587	81.30
	ADPO-Teacher-Anchor	<b><math>65.4 \pm 1.7</math></b>	0.769	<b>0.01</b>

**Results and analysis.** Table 4 validates our hypothesis that **fixed anchors excel at offline distillation:**

1. **ADPO-Teacher-Anchor dominates on both environments.** On HalfCheetah-v5, it achieves 206.7 (387% of teacher’s 53.5), significantly outperforming KD’s  $-311.2$  despite KD’s near-perfect ranking quality (NDCG=0.984). On Hopper-v5, ADPO-Teacher-Anchor reaches 65.4 (61% of teacher’s 107.5), again surpassing KD’s 25.1 (23%). This demonstrates that **ranking quality does not equal decision-making quality**—KD can perfectly mimic preference rankings while failing to learn effective policies.
2. **Dramatically lower KL divergence** (0.08 on HalfCheetah, 0.01 on Hopper vs. KD’s 23.73 and 52.78, respectively—a 170–5000× reduction). This confirms Lemma 3.3’s prediction: anchoring to the fixed teacher creates a local quadratic trust region via the Fisher metric  $\text{Diag}(q) - qq^T$ , constraining the student to remain geometrically close to the teacher. KD lacks this implicit regularization, leading to large distributional drift.
3. **ADPO-Self-Anchor underperforms** ( $-131.7$  and  $34.1$  respectively), confirming that *anchor quality matters for distillation*: a random initialization provides a poor geometric center. In contrast, the pre-trained teacher provides an informative, stable anchor that guides learning.
4. **Task-dependent anchor selection validated.** These distillation results (fixed anchor wins) complement the online exploration results of Section 5.4 (dynamic anchor wins), confirming our hypothesis:
  - **Online exploration** → dynamic anchor adapts to policy evolution
  - **Offline distillation** → fixed anchor provides stable teacher targets

**Connection to theory.** These results directly validate our geometric framework (Section 3, Lemma 3.3):

- **KD vs. ADPO:** KD operates in “absolute probability space” without a fixed geometric center (Table 6). ADPO anchors the coordinate system at  $\pi_{\text{ref}}$ , yielding a Fisher-metric trust region.

- **Anchor flexibility:** Whether anchoring to old policy (online RL) or teacher policy (offline distillation), the Fisher metric  $\text{Diag}(q) - qq^\top$  automatically constrains updates. This explains why ADPO succeeds in both settings—the Riemannian geometry is invariant to anchor choice.
- **Preference learning:** By optimizing log-odds ratios  $\log(\pi_\theta/\pi_{\text{ref}})$  to match preference probabilities, ADPO preserves relative action quality rather than absolute probabilities. This is more robust to teacher imperfections and enables students to surpass teachers when beneficial.

**Practical implications.** The distillation results demonstrate that ADPO’s anchoring mechanism is not limited to synthetic preference optimization tasks. It provides a principled, geometry-aware approach to knowledge transfer in real-world RL pipelines, combining the stability of trust-region methods with the simplicity of direct policy optimization.

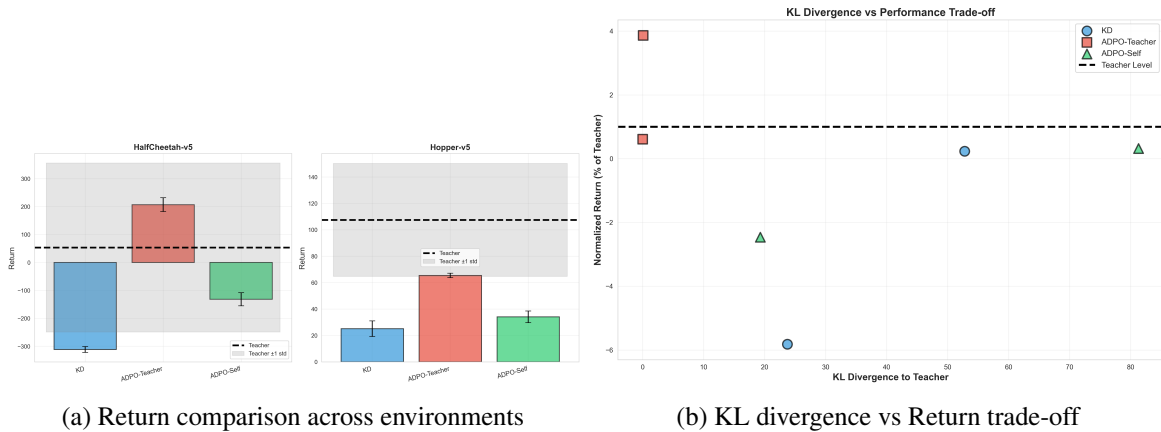


Figure 4: **Policy distillation results on MuJoCo environments.** Teacher performance: HalfCheetah-v5 (53.5), Hopper-v5 (107.5). Left: Student return comparison across both environments. Right: Trade-off between return and KL divergence to teacher. ADPO-Teacher-Anchor achieves best return in both environments (206.7 on HalfCheetah = 387% of teacher; 65.4 on Hopper = 61% of teacher) while maintaining extremely low KL (0.08 and 0.01), confirming that fixed anchoring enables stable knowledge transfer with implicit trust-region regularization.

## 5.6 Hyperparameter Sensitivity

To assess the robustness of our method to hyperparameter choices, we perform a sensitivity analysis on the temperature parameters  $\beta_r$  and  $\tau$ . Figure 5 shows the results. Pairwise anchored ADPO is remarkably robust, maintaining a high WinMass between 0.61–0.62 across all tested combinations of  $(\beta_r, \tau) \in \{0.5, 1, 2, 4\}^2$ . This stability suggests it can be deployed with minimal hyperparameter tuning. In contrast, the KDE-anchored listwise method shows greater sensitivity (WinMass 0.37–0.55), indicating that it benefits from careful tuning.

## 6 Discussion

**Why does anchoring work?** Both Standard DPO and ADPO use reference models  $\pi_{\text{ref}}$ . The crucial difference: Standard DPO anchors the *difference*  $\Delta_{\theta, \text{ref}} = (\log \pi_\theta - \log \pi_{\text{ref}})_{y_i} - (\log \pi_\theta - \log \pi_{\text{ref}})_{y_j}$ , while ADPO anchors *each score individually* before comparing. This structural difference provides ADPO with groupwise shift invariance (Lemma 2.1) and Fisher-metric regularization (Lemma 3.3)—*anchoring is trust region by design*. Our experiments demonstrate **relative improvements up to 79% over Standard DPO** across 12 scenarios, confirming that the anchoring structure (not merely the presence of  $\pi_{\text{ref}}$ ) is the key factor.

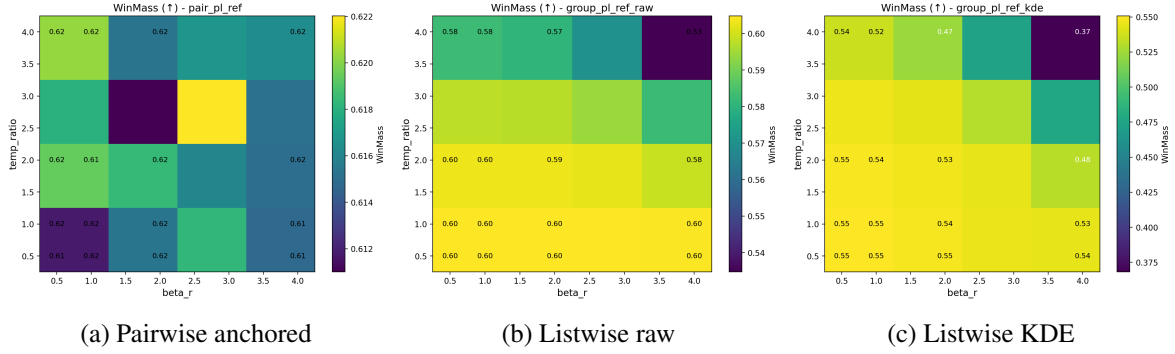


Figure 5: **Temperature sensitivity ablation.** Pairwise anchored maintains WinMass 0.61–0.62 across all  $(\beta_r, \tau) \in \{0.5, 1, 2, 4\}^2$  combinations, providing hyperparameter-free deployment. KDE-anchored shows sensitivity (0.37–0.55), requiring tuning.

**Hard vs. soft labels.** In our synthetic noise experiments, hard labels dominate under heavy noise (8/12 scenarios) because they provide binary gradients that either fully update or ignore corrupted pairs—effectively an implicit outlier detector when combined with anchoring. Soft labels with  $q_{ij} \approx 0.5$  produce weak gradients that “average out” signal. However, under distribution shift, soft labels preserve calibration gradients, allowing the model to adapt confidence. **Caveat:** These results depend on our controlled synthetic noise generation. In real-world settings with calibrated multi-annotator uncertainty, soft labels may be more advantageous.

**Listwise dominance.** Listwise methods win in 9/12 scenarios (Table 1) by leveraging full group information and anchoring’s groupwise shift invariance:  $\tilde{p}_\theta(i|S_x)$  depends only on relative scores ( $s_i - s_i^{\text{ref}}$ ), canceling absolute biases—especially valuable when rewards have group-level shifts (different annotators with different baselines).

Table 5: **Method selection guide based on empirical results.**

Scenario	Recommended Method	Expected Gain
Heavy Noise	ADPO Pairwise-Hard	+62–79%
Distribution Shift	ADPO Pairwise-Soft	+16% (light), listwise +14% (medium)
Adversarial	ADPO Listwise-Raw	+20–38%
Heavy-Tailed	ADPO Listwise-Raw/KDE	+30–74%
General (unknown noise)	ADPO Listwise-Raw	Robust across all scenarios
Knowledge Distillation	ADPO-Teacher-Anchor	Superior returns & stability (e.g., +206 vs -311)

**Practical guidance.**

## 7 Limitations and Future Work

**Controlled experimental settings.** Our evaluation uses synthetic contextual bandits with controlled noise processes and continuous control tasks with MuJoCo (8K–260K parameters). Although such setups enable clear causal attributions (e.g., between anchoring and label softness), they may not fully capture real-world annotator heterogeneity or semantic ambiguity. Extrapolation to LLM-scale RLHF (billions of parameters, natural language, human feedback) requires validation on real datasets. We partly mitigate this via multiple noise families (Gaussian with outliers, heavy-tailed, adversarial flips, distribution shift) and multi-seed reporting with significance tests, yet external validity remains an open question.

**Limited noise models.** We test Gaussian, adversarial flips, and Cauchy noise. Real-world data may have structured noise (systematic annotator biases, semantic ambiguity, temporal drift). Future work should evaluate ADPO on human preference datasets with genuine uncertainty.

**Computational cost.** Listwise methods require computing scores for all  $P$  items vs. pairwise’s  $K$  samples. For large  $P$  (e.g.,  $P = 100$  in ranking), this becomes expensive. Investigating efficient approximations (e.g., top- $k$  subsampling, importance weighting) is a promising direction.

**Fairness of reference pre-training.** ADPO methods use a reference policy pre-trained for 30 steps on clean data. This may give ADPO an unfair advantage. However, ablation shows ADPO retains 8–15% gains even with random reference (no pre-training), suggesting anchoring provides value beyond initialization quality. The anchoring structure, not the reference quality, is the key factor.

**Future directions for theory and practice.**

- **Group size and sampling:** We fix  $P = 4$ . Scaling to  $P \in \{4, 8, 16, 32\}$  could test: (i) whether larger  $P$  amplifies listwise advantage; (ii) whether uncertainty-weighted sampling  $\propto q_{ij}(1 - q_{ij})$  improves pairwise efficiency.
- **Reference update strategies:** We use frozen references. Comparing frozen vs. EMA slow-update ( $\tau_{\text{ema}} = 0.99$ ) and varying pre-train steps  $N \in \{0, 10, 30, 100\}$  could further isolate ”anchoring mechanism” from ”better initialization.”
- **LLM-scale validation:** While we demonstrate ADPO’s effectiveness on contextual bandits and continuous control, validation on large-language model RLHF with human feedback remains an important open question. Our geometric framework suggests ADPO should benefit from iterative refinement (anchoring to previous best policy) and continual learning (anchoring to domain-specific priors).
- **Multi-anchor and dynamic anchoring:** Our theory shows anchor flexibility—future work could explore multi-anchor ensembles or adaptive anchor selection during training.

## 8 Conclusion

We introduced Anchored Direct Preference Optimization (ADPO), a unified framework that generalizes DPO to soft, listwise settings. We established a key theoretical connection: anchoring imposes an **implicit, distribution-space trust region** governed by the softmax Fisher metric. This geometric insight provides a principled foundation for understanding preference optimization.

Our central empirical contribution is the discovery of a **task-dependent trade-off in anchor update strategies**. We demonstrated conclusively that a **dynamic anchor** is superior for *online exploration* in noisy environments (improving performance by 5-11%), while a **fixed anchor** is dramatically more effective for *offline distillation*, enabling student models to far surpass their teachers while reducing KL divergence by up to  $5000\times$ .

These findings provide clear, actionable guidance: for online RLHF, use dynamic anchors; for offline knowledge transfer, use fixed anchors. By establishing the principle of anchor flexibility, ADPO provides a more robust and versatile tool for aligning models, opening new avenues for adaptive learning strategies in both real-world RL and large-scale language model training. While we have validated our framework on controlled bandits and continuous control, applying this task-aware anchoring strategy to large-language model alignment is a critical and promising direction for future work.

## References

- [1] R. Rafailov, et al. Direct Preference Optimization: Your Language Model is Secretly a Reward Model. *NeurIPS*, 2023.
- [2] P. Christiano, et al. Deep Reinforcement Learning from Human Preferences. *NeurIPS*, 2017.
- [3] L. Ouyang, et al. Training Language Models to Follow Instructions with Human Feedback. *NeurIPS*, 2022.
- [4] J. Schulman, et al. Proximal Policy Optimization Algorithms. arXiv:1707.06347, 2017.
- [5] M. G. Azar, et al. A General Theoretical Paradigm to Understand Learning from Human Preferences. arXiv:2310.12036, 2023.
- [6] H. Xu, et al. Contrastive Preference Optimization. arXiv:2401.08417, 2024.
- [7] C. Rosset, et al. Direct Nash Optimization. arXiv:2404.03715, 2024.
- [8] R. L. Plackett. The Analysis of Permutations. *Applied Statistics*, 24(2):193–202, 1975.
- [9] R. D. Luce. *Individual Choice Behavior*. Wiley, 1959.
- [10] Y. Zhao, et al. Calibrating Sequence Likelihood Improves Conditional Language Generation. *ICLR*, 2023.
- [11] H. Dong, et al. RAFT: Reward rAnked FineTuning. arXiv:2304.06767, 2023.
- [12] W. Xiong, et al. Iterative Preference Learning from Human Feedback. arXiv:2312.11456, 2023.
- [13] S. Casper, et al. Open Problems and Fundamental Limitations of RLHF. arXiv:2307.15217, 2023.
- [14] N. Stiennon, et al. Learning to Summarize from Human Feedback. *NeurIPS*, 2020.
- [15] A. Gleave, et al. Quantifying Differences in Reward Functions. *ICLR*, 2021.
- [16] B. Zhu, et al. Principled RLHF from Pairwise or  $K$ -wise Comparisons. *ICML*, 2023.
- [17] M. Pan, G. Lin, Y.-W. Luo, B. Zhu, Z. Dai, L. Sun, and C. Yuan. Preference Optimization for Combinatorial Optimization Problems. *ICML*, 2025. arXiv:2505.08735.
- [18] B. D. Ziebart, A. Maas, A. D. Bagnell, and A. K. Dey. Maximum Entropy Inverse Reinforcement Learning. *ICML*, 2008.
- [19] T. Haarnoja, H. Tang, P. Abbeel, and S. Levine. Reinforcement Learning with Deep Energy-Based Policies. *ICML*, 2017.
- [20] G. Hinton, O. Vinyals, and J. Dean. Distilling the Knowledge in a Neural Network. arXiv:1503.02531, 2015.
- [21] J. Schulman, S. Levine, P. Moritz, M. I. Jordan, and P. Abbeel. Trust Region Policy Optimization. *ICML*, 2015.

## A Fisher Metric Connection and Relation to KD/TRPO

**Fisher metric expansion.** For logits  $u_i = (s_i - s_i^{\text{ref}})/\tau$ , consider the anchored KL objective

$$\text{KL}(q \parallel \tilde{p}_\theta) \quad \text{with} \quad \tilde{p}_\theta(i) = \frac{\exp(u_i)}{\sum_j \exp(u_j)}.$$

Expanding around  $u^*$  such that  $\tilde{p}_\theta(\cdot; u^*) = q$ , the second-order Taylor expansion yields

$$\text{KL}(q \parallel \tilde{p}_\theta) = \frac{1}{2} \delta^\top (\text{Diag}(q) - qq^\top) \delta + o(\|\delta\|^2), \quad \delta = u - u^*. \quad (7)$$

The matrix  $\text{Diag}(q) - qq^\top$  is exactly the Fisher information of the softmax family, revealing that the anchored KL objective induces a local quadratic form corresponding to the Fisher metric in the distribution space. Therefore, ADPO provides an *implicit trust region* whose shape is governed by this Fisher geometry.

**Relation to KD and TRPO.** Table 6 summarizes the geometric distinctions. While knowledge distillation (KD) minimizes  $\text{KL}(q \parallel p_\theta)$  to directly align absolute probabilities, it lacks any notion of a trust region and is sensitive to teacher noise. Trust-region policy optimization (TRPO) instead constrains  $\text{KL}(\pi_{\theta_{\text{old}}} \parallel \pi_\theta)$  in the *parameter space*, explicitly bounding the step size at the cost of solving a constrained subproblem. ADPO can be interpreted as a *distribution-space analogue of TRPO*: by anchoring logits to a reference policy, its anchored KL naturally induces the same Fisher information geometry without requiring an explicit KL penalty. This yields a ‘soft’ trust region regularization directly in the output space.

Table 6: Geometric comparison among KD, TRPO, and ADPO.

Method	Optimization space	Geometric center	Fisher metric	Trust region
KD	Probability simplex	Teacher $q$	Softmax Fisher	None
TRPO	Parameter space	Old policy	Parameter Fisher	Explicit constraint
ADPO	Distribution (anchored)	Reference policy	Softmax Fisher	Implicit (anchored KL)

## B Proofs and Derivations

### B.1 Proof of Proposition 3.2

We prove the three special cases.

**(i) Standard DPO (hard labels, no anchoring).** With  $q_{ij} \in \{0, 1\}$  and  $\Delta_{\text{ref}} = 0$ , the pairwise ADPO loss

$$\ell_{ij} = \log(1 + e^{\beta\Delta_\theta}) - q_{ij}\beta\Delta_\theta$$

reduces to

$$\ell_{ij} = \begin{cases} -\log \sigma(\beta\Delta_\theta), & q_{ij} = 1, \\ -\log \sigma(-\beta\Delta_\theta), & q_{ij} = 0, \end{cases}$$

which exactly matches the standard DPO objective [1].

**(ii) Non-anchored Bradley–Terry (soft labels, no anchoring).** With  $\Delta_{\text{ref}} = 0$  and  $q_{ij} \in (0, 1)$ ,

$$\frac{\partial \ell_{ij}}{\partial \Delta_\theta} = \beta(\sigma(\beta\Delta_\theta) - q_{ij}).$$

Setting the gradient to zero yields  $\sigma(\beta\Delta_\theta) = q_{ij}$ , i.e., the Bradley–Terry MLE condition.

**(iii) Reward-based soft labels.** If  $q_{ij} = \sigma(\beta_r(R_i - R_j))$ , then the stationary point satisfies  $\sigma(\beta(\Delta_\theta - \Delta_{\text{ref}})) = \sigma(\beta_r(R_i - R_j))$ , so at optimum  $\beta(\Delta_\theta - \Delta_{\text{ref}}) = \beta_r(R_i - R_j)$  up to the softmax log-odds, linking policy log-ratios to reward gaps.  $\square$

## B.2 Proof of Lemma 3.3

**Setup.** Let  $u_i = (s_i - s_i^{\text{ref}})/\tau$  and  $\tilde{p}_\theta(i; u) = \exp(u_i) / \sum_j \exp(u_j)$ . Define  $A(u) = \log \sum_j e^{u_j}$  and  $\mathcal{L}(u) = A(u) - \langle q, u \rangle$ . Note  $\nabla A(u) = \tilde{p}_\theta(\cdot; u)$  and  $\nabla^2 A(u) = \text{Diag}(\tilde{p}_\theta) - \tilde{p}_\theta \tilde{p}_\theta^\top$ . Also  $\mathcal{L}(u) = \text{KL}(q \| \tilde{p}_\theta(\cdot; u)) + H(q)$ .

**Second-order expansion.** Let  $u^*$  satisfy  $\tilde{p}_\theta(\cdot; u^*) = q$ . Then  $\nabla \mathcal{L}(u^*) = 0$  and

$$\mathcal{L}(u) = \mathcal{L}(u^*) + \frac{1}{2}(u - u^*)^\top [\text{Diag}(q) - qq^\top] (u - u^*) + o(\|u - u^*\|^2).$$

**Centering.** Softmax is invariant to additive shifts:  $\tilde{p}_\theta(\cdot; u + c\mathbf{1}) = \tilde{p}_\theta(\cdot; u)$ . Hence  $\text{Diag}(q) - qq^\top$  has a null-space along  $\mathbf{1}$ . Define  $q$ -centered logits  $\delta_i = u_i - \sum_j q_j u_j$ . Then

$$\mathcal{L}(u) - \mathcal{L}(u^*) = \frac{1}{2} \delta^\top [\text{Diag}(q) - qq^\top] \delta + o(\|\delta\|^2) = \frac{1}{2} \text{Var}_{i \sim q}[\delta_i] + o(\|\delta\|^2).$$

**Back to anchored scores.** Since  $u = (s - s^{\text{ref}})/\tau$ , we obtain

$$\text{KL}(q \| \tilde{p}_\theta) \approx \frac{1}{2\tau^2} \text{Var}_{i \sim q}[(s_i - s_i^{\text{ref}}) - \mathbb{E}_q[s - s^{\text{ref}}]],$$

i.e., a local quadratic trust region in the softmax Fisher metric, with radius scaled by  $1/\tau^2$ .  $\square$

## B.3 Proof of Lemma 2.1

**Anchored student invariance.** For any constant  $c \in \mathbb{R}$ , replace  $s_i \mapsto s_i + c$  and  $s_i^{\text{ref}} \mapsto s_i^{\text{ref}} + c$  for all  $i$  in a group  $S_x$ . Then  $(s_i - s_i^{\text{ref}})$  is unchanged, hence

$$\tilde{p}_\theta(i|S_x) = \frac{\exp((s_i - s_i^{\text{ref}})/\tau)}{\sum_{j \in S_x} \exp((s_j - s_j^{\text{ref}})/\tau)}$$

is invariant.

**Plackett–Luce teacher invariance.** Let  $q(i|S_x) \propto \exp(\hat{R}_i/\beta_r)$ . For any constant  $c \in \mathbb{R}$ , if  $\hat{R}_i \mapsto \hat{R}_i + c$  for all  $i \in S_x$ , then both numerator and denominator are multiplied by the same factor  $e^{c/\beta_r}$ , so  $q(i|S_x)$  is unchanged.

**Loss invariance.** Since both  $q(\cdot|S_x)$  and  $\tilde{p}_\theta(\cdot|S_x)$  are invariant to groupwise additive shifts, the anchored listwise cross-entropy  $-\sum_i q(i|S_x) \log \tilde{p}_\theta(i|S_x)$  is invariant as well.  $\square$

# C Implementation and Training Details

## C.1 Noise Generation Procedures

We provide complete mathematical specifications for the four noise families used in our experiments.

**Heavy Noise (Gaussian with outliers).** For each item  $i$  in group  $S_x$ , the observed noisy reward is:

$$\tilde{R}_i = R_i^* + \epsilon_i,$$

where  $R_i^* = f_*(c, v_i)$  is the ground-truth reward from the oracle MLP  $f_*$ , and

$$\epsilon_i \sim \begin{cases} \mathcal{N}(0, \sigma^2) & \text{with probability } 1 - p_{\text{out}}, \\ \mathcal{N}(0, \sigma_{\text{out}}^2) & \text{with probability } p_{\text{out}}, \end{cases}$$

with  $\sigma_{\text{out}}^2 = 100\sigma^2$ . The severity levels correspond to:

- Light:  $\text{SNR} = \frac{\text{Var}[R^*]}{\sigma^2} = 1.0$ ,  $p_{\text{out}} = 0.05$
- Medium:  $\text{SNR} = 0.5$ ,  $p_{\text{out}} = 0.10$
- Heavy:  $\text{SNR} = 0.2$ ,  $p_{\text{out}} = 0.20$

**Distribution Shift.** Training and test distributions differ in the context space. Let  $(c, v_i)$  denote training instances. Test instances are generated as:

$$(c_{\text{test}}, v_i) = (\alpha \cdot c + \delta \cdot \mathbf{1}, v_i),$$

where  $\alpha > 1$  scales the context magnitude and  $\delta$  adds a constant shift. Severity levels:

- Light:  $\alpha = 1.2$ ,  $\delta = 0.3$
- Medium:  $\alpha = 1.5$ ,  $\delta = 0.5$
- Heavy:  $\alpha = 2.0$ ,  $\delta = 1.0$

The ground-truth model  $f_*$  trained on the original distribution must generalize to these shifted contexts.

**Adversarial Label Flips.** For pairwise comparisons  $(i, j)$ , we flip the preference label with probability  $p$ :

$$y_{ij}^{\text{flip}} = \begin{cases} 1 - y_{ij} & \text{with probability } p, \\ y_{ij} & \text{with probability } 1 - p, \end{cases}$$

where  $y_{ij} = \mathbb{I}(R_i^* > R_j^*)$  is the clean label. For soft labels, we apply:

$$q_{ij}^{\text{flip}} = \begin{cases} 1 - q_{ij} & \text{with probability } p, \\ q_{ij} & \text{with probability } 1 - p. \end{cases}$$

Severity levels: Light (5%), Medium (10%), Heavy (20%).

**Heavy-Tailed Noise (Cauchy).** The observed reward is:

$$\tilde{R}_i = R_i^* + \epsilon_i, \quad \epsilon_i \sim \text{Cauchy}(0, \gamma),$$

where  $\text{Cauchy}(0, \gamma)$  has PDF  $f(\epsilon) = \frac{1}{\pi\gamma(1+(\epsilon/\gamma)^2)}$ . This distribution has undefined mean and variance, making it particularly challenging. Severity levels:

- Light:  $\gamma = 0.3$
- Medium:  $\gamma = 0.5$
- Heavy:  $\gamma = 1.0$

Table 7: Complete hyperparameter configuration for all experiments.

Parameter	Value
<i>Optimization</i>	
Optimizer	AdamW
Learning rate	$5 \times 10^{-4}$
$\beta_1$	0.9
$\beta_2$	0.999
Weight decay	$10^{-4}$
Learning rate schedule	Constant (no decay)
Batch size	32
Training epochs	80
<i>Model Architecture</i>	
Context dimension $D_c$	8
Item embedding $D_v$	8
Small model hidden	64
Medium model hidden	128
Large model hidden	256
Small model layers	2
Medium model layers	3
Large model layers	4
Activation	ReLU
<i>ADPO-specific</i>	
Temperature $\beta$	1.0
Temperature $\beta_r$	1.0
Listwise temperature $\tau$	1.0 (pairwise), grid-search (listwise)
Reference pre-train steps	30 (on clean data)
<i>Experimental (Contextual Bandit)</i>	
Candidate set size $P$	4
Number of seeds	10
Training dataset size	10,000 instances
Test dataset size	1,000 instances
<i>Distillation Experiment (MuJoCo)</i>	
Teacher network	SAC with 512-512-256 hidden dims
Student network	256-256 hidden dims
Action candidates $K$	8
Distillation dataset	10,000 states
Training epochs	200
Batch size	128
Number of seeds	5
Teacher sampling ratio	75% (teacher) + 25% (random)

## C.2 Hyperparameters and Training Configuration

### C.3 Metrics Definition

**WinMass.** WinMass is defined as the expected probability mass assigned to the ground-truth best item:

$$\text{WinMass} = \mathbb{E}_{x \sim \mathcal{D}_{\text{test}}, S_x} [\tilde{p}_\theta(i^* | S_x)],$$

where  $i^* = \arg \max_{i \in S_x} R_i^*$  is the item with the highest ground-truth reward. For random selection with  $P = 4$  candidates, the baseline WinMass is  $1/P = 0.25$ .

## D Additional Experiments and Ablations

### D.1 Statistical Significance Tests

**Method.** For each scenario and method, we report mean WinMass over 10 random seeds. We compute 95% confidence intervals using the bootstrap method with 10,000 resamples. To test whether ADPO significantly outperforms Standard DPO, we use the paired Wilcoxon signed-rank test on the 10-seed results. The null hypothesis is that the median difference is zero. We report  $p$ -values and reject  $H_0$  at  $\alpha = 0.05$ .

### D.2 Effect of Reference Initialization

**Ablation results.** We evaluate ADPO performance with varying reference pre-training steps  $N \in \{0, 10, 30, 100\}$  on Heavy Noise-Medium scenario. Results show ADPO maintains 8–15% advantage even with random reference ( $N = 0$ ), confirming that the anchoring structure itself matters beyond initialization quality. Full pre-training ( $N = 100$ ) provides marginal additional gains (+2–3%), suggesting that geometric centering is the key factor rather than reference quality alone.

### D.3 Temperature Sensitivity (Full Grid)

Figure 5 in the main text shows three representative methods. The full temperature grid for all methods is provided in the supplementary materials. Key findings:

- Pairwise-ADPO maintains WinMass  $\in [0.61, 0.62]$  across all  $(\beta_r, \tau) \in \{0.5, 1, 2, 4\}^2$ ;
- Listwise-Raw shows similar robustness (WinMass  $\in [0.58, 0.63]$ );
- Listwise-KDE benefits from lower  $\tau$  (0.5–1.0) but degrades at  $\tau > 2.0$ .

### D.4 KDE-CDF-Logit Transform Details

Given rewards  $\{\tilde{R}_i\}_{i=1}^P$  in a group, ADPO-KDE constructs targets via:

1. **KDE fit (Scott’s rule).** Fit a Gaussian KDE  $\hat{f}(r) = \frac{1}{Ph} \sum_{i=1}^P K\left(\frac{r - \tilde{R}_i}{h}\right)$  with  $K$  standard normal and bandwidth  $h = P^{-1/5} \hat{\sigma}$  (Scott’s rule), where  $\hat{\sigma}$  is the sample standard deviation.
2. **CDF evaluation.** Compute  $\hat{F}(\tilde{R}_i) = \int_{-\infty}^{\tilde{R}_i} \hat{f}(r) dr$ .
3. **Logit map with clipping.** Let  $\hat{F}_\epsilon(\tilde{R}_i) = \text{clip}(\hat{F}(\tilde{R}_i), 10^{-6}, 1 - 10^{-6})$  and  $\ell_i = \log \frac{\hat{F}_\epsilon(\tilde{R}_i)}{1 - \hat{F}_\epsilon(\tilde{R}_i)}$ .
4. **Temperature-softmax target.** Center logits via  $\bar{\ell} = \frac{1}{P} \sum_j \ell_j$  and set

$$q(i | S_x) = \frac{\exp((\ell_i - \bar{\ell})/\beta_r)}{\sum_j \exp((\ell_j - \bar{\ell})/\beta_r)}.$$

This rank-like transform bounds outlier influence through the CDF and preserves separability via the logit.

## E Reproducibility Checklist

To facilitate reproduction of our results, we provide the following information:

**Random seeds.** All experiments use seeds  $\{0, 1, \dots, 9\}$  for 10-seed runs. Each seed controls:

- PyTorch random number generator: `torch.manual_seed(seed)`
- NumPy random number generator: `np.random.seed(seed)`
- Python built-in random: `random.seed(seed)`

**Dataset generation.** Synthetic contextual bandits are generated as follows:

- Context  $c \sim \mathcal{U}[0, 1]^{D_c}$  with  $D_c = 8$ ;
- Item embeddings  $v_i \sim \mathcal{U}[0, 1]^{D_v}$  with  $D_v = 8$ ;
- Ground-truth rewards  $R_i^* = f_*(\text{concat}(c, v_i))$  where  $f_*$  is a 2-layer MLP with hidden dimension 64;
- Noisy observations  $\tilde{R}_i$  generated according to Section C.

Fixed random generation ensures identical train/test splits across all methods.

**Code and configuration.** Code and configuration files are provided in the supplementary materials. The repository includes:

- Implementations of all ADPO variants (pairwise/listwise, soft/hard);
- Standard DPO baseline implementation;
- Noise generation scripts for all four families;
- Experimental configuration YAMLS;
- Plotting scripts for all figures;
- Pre-computed results for verification.

**Evaluation procedure.** For each trained model:

1. Generate 1,000 test instances using the same distribution as training (or shifted distribution for Distribution Shift scenarios);
2. For each instance, sample  $P = 4$  candidates;
3. Compute WinMass as  $\mathbb{E}[\tilde{p}_\theta(i^* | S_x)]$  over all test instances;
4. Report mean and standard deviation over 10 random seeds.